Journal of Himalayan Earth Sciences Volume 53, No. 2, 2020 pp. 34-51

Detrital modes in Lower Mesozoic sandstone of the Wulgai Formation (Pakistan): implications for provenance

Muhammad Ismail[1], Aimal Khan Kasi[1*], Razzaq Abdul Manan[1], Mohibullah Mohibullah[2] and Nisar Ahmed[3]

[1] Centre of Excellence in Mineralogy, University of Balochistan, Pakistan

[2] Department of Geology, University of Balochistan, Pakistan

[3] Geological Survey of Pakistan, Quetta

**Corresponding author's email: aimal_kasi@yahoo.co.uk*

Submitted date:10/05/2020 Accepted date:14/07/2020 Published online:

Abstract

The detrital modes of twenty-five sandstone samples from Triassic Wulgai Formation have been studied in Zhob and Qila Saifullah districts of Balochistan province in order to determine their provenance and tectonic setting. The sandstone is mostly fine- to medium-grained. Quartz is the most abundant framework grain in sandstone, while heavy minerals include rutile, tourmaline, staurolite, zircon, and hornblende. Among the lithic fragments, metamorphic lithic fragments are the most abundant rock fragments. The sandstone of the Wulgai Formation is classified as quartz arenite (Q96F4L0.2). The Qt-F-L (Qt96F4L0.2) and Qm-F-Lt (Qm96F3Lt1) plots show the craton interior as the source terrain for the sandstone, in which metamorphic and plutonic terrains were the most dominant sources. The very-high content of monocrystalline quartz indicates high maturity of the sandstone, which may be attributed to quartz-rich, acidic igneous and high-grade metamorphic terrains. The most quartzose sands are usually derived from stable craton interiors having low relief.

Keywords: Triassic, Wulgai Formation, Sulaiman Belt, Indian Plate, Detrital modes, Craton Interior

1. Introduction

Mesozoic rocks of Pakistan show great variation in lithology and thickness and are widely exposed across the country. Mesozoic rocks are also well exposed in the Kirthar and Sulaiman Fold-Thrust belts (KSFTBs) in Balochistan and attain thicknesses of over thousands of meters (Fig 1). Disconformities between the Triassic and Jurassic successions are not very pronounced in KSFTB as in the northern belts of Pakistan, and in many cases, the sedimentation is believed to have been unhindered throughout Triassic and Jurassic periods (Fatmi, 1977; Manan, 2014). The Hunting Survey Corporation (HSC; Jones, 1961) mapped and described for the first time the Triassic succession of the Sulaiman Fold-Thrust Belt (Wulgai Formation). Later Maldonado et al. (2011) modified and digitized the HSC map (Jones, 1961) at a 1:250,000 scale, covering the entire belt. The Triassic Wulgai Formation is largely composed of thin to medium limestone interbedded with shale and occasionally sandstone beds (Manan, 2014). The study area falls in the western part of the Sulaiman Fold-thrust Belt (SFTB) (Figs 1 and 2), where a Triassic-to-Pleistocene sedimentary and volcanogenic succession crops out (Table 1) (Kassi et al., 2009). These rocks are exposed in a series of E-W and ENE-WSW trending, thrust-bound, folds (Jadoon et al., 1994; Reynolds, 2015). The stratigraphic framework and tectonic history of the area are the result of the India's rifting from Gondwana, drifting and collision with Asia (Powell, 1979; Brookfield, 1993; Beck et al., 1995; Hodges, 2000). Deposition of marine sediments (now exposed in the SFTB) took place on the western margin of the Indian Plate in Paleo- and Neo-Tethys before and after its separation from Afro-Arabian Plate (Manan et al., 2012); the ten kilometers-thick successions accumulated during the pre-rift, syn-rift and drift phases (Jones, 1961; Kassi et al., 2009).

Triassic Wulgai Formation, is the oldest formation exposed in the Sulaiman and Kirthar ranges (Jones, 1961). It is estimated to be 1180 m thick in the type section (Wulgai, Khanozai area – Williams, 1959). The main lithologies are the limestone and the shale. Manan et al. (2012) described for the first time sandstone embedded in the Wulgai Formation from the

Feroz-e-Kan (Nisai area) and Ziarat Morh (Quetta-Ziarat road junction) sections in the western Sulaiman Fold-Thrust Belt.

This work studies the composition and detrital modes of sandstone in the Wulgai Formation in SFTB (Qila Saifullah and Zhob districts) in order to determine the provenance and tectonic setting of the source area. A number of studies have proposed the Indian shield as the source terrain for the siliciclastic component of the Jurassic-Upper Cretaceous succession (Manan et al., 2012; Kassi et al., 1991; Sultan and Gipson, 1995; Umar et al., 2011). However, Indian shield has not been assessed as a possible source area for the sandstone of the Triassic Wulgai Formation.

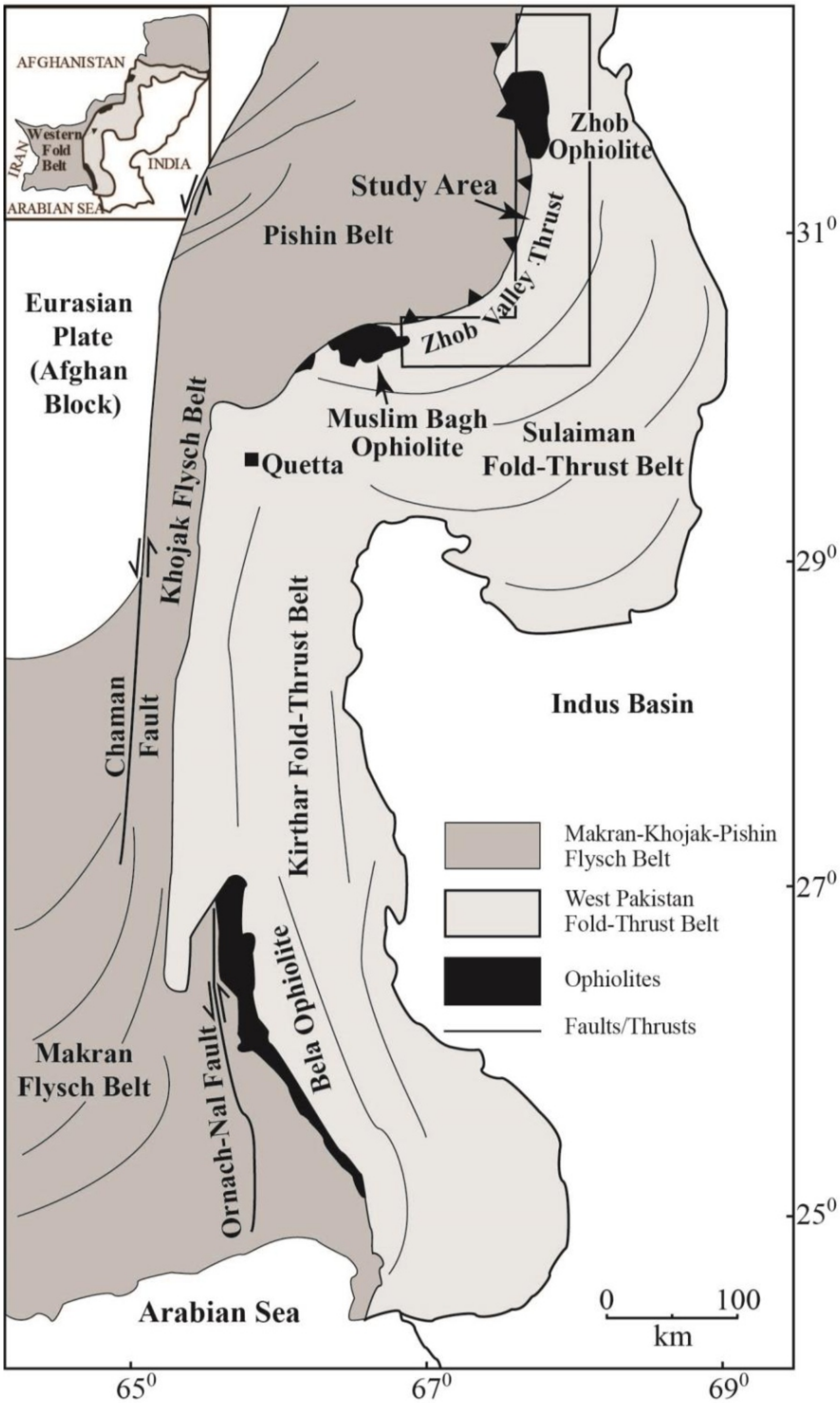

Fig. 1. Generalized geological map of the western part of Pakistan showing the position of the Pishin Belt and of the study area (modified after Bender and Raza, 1995).

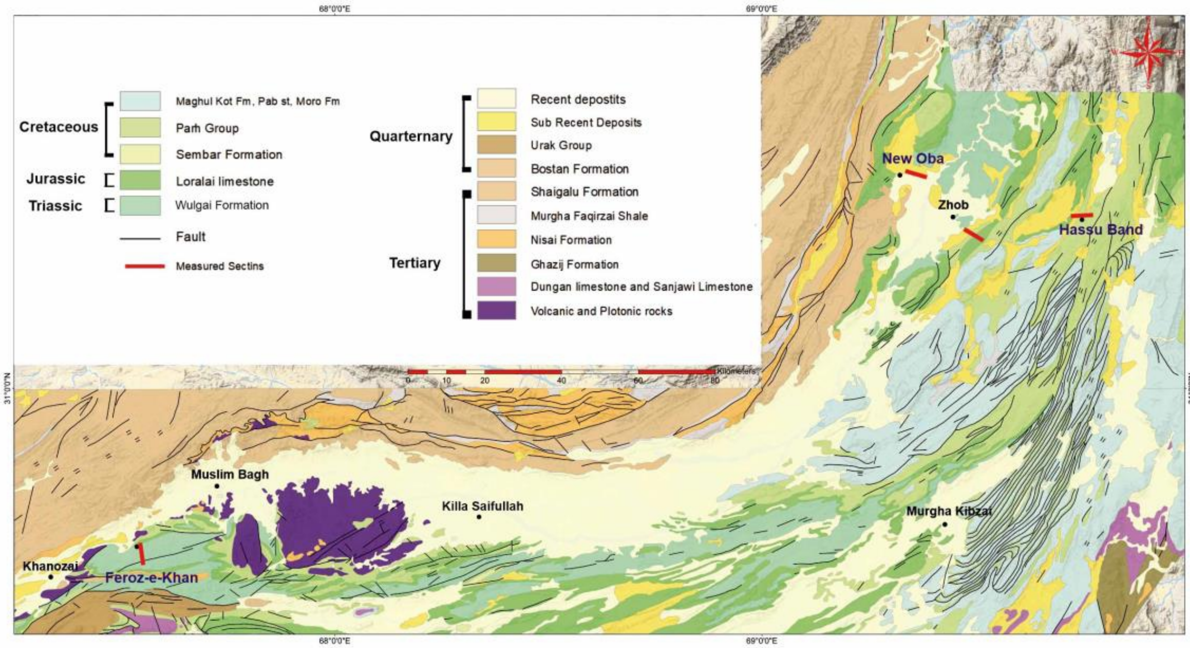

Fig. 2. Geological map of the study area showing the Triassic-Pleistocene rocks of the western Sulaiman Fold-Thrust Belt (modified after Jones, 1961).

2. Geological setting

About 170 million years ago (my) the Indian Plate detached from Gondwana Supercontinent and started drifting towards Eurasia (Powell, 1979; Chatterjee et al., 2013). It collided with the Kohistan Island Arc around 55 my, and later with the stationary Eurasian Plate occurred about 30 my (Searel et al., 1997; Copley et al., 2010). This led to the closure of the northern part of the Neo Tethys Ocean in the Eocene/Oligocene and the opening of the remnant ocean in the southwest (Katawaz remnant ocean), which remained open up to the Miocene (Qayyum et al., 2001). The collision of India with Eurasia produced uplfting, folding and thrusting, and led to the formation of the Himalayan Mountain Chain and the KSFTBs. The latter represent the southwest branch of the Himalayas, (Davy and Cobbold, 1988; Klootwijket et al., 1994; Haq and Davis, 1997; Iqbal and Khan, 2012). The Bela-Waziristan Ophiolite belt borders the KSFTBs to the west, and further westward flysch-molasse sediments of the Katawaz basin are exposed. The Indian Plate is bounded to the west by the Chaman transform boundary with its major faults (i.e. Chaman, Ghazaband and Ornach-Nal faults), which truncates the Katawaz basin, and to the east by the Indus Plain.

The SFTB is the southwestern extension of the Himalayan belt in Pakistan (Bannert et al., 1993; Jadoon et al., 1994; Bender and Raza, 1995; Jadoon and Khurshid, 1996; Kazmi and Jan, 1997). The SFTB is bounded to the west by Zhob valley ophiolite and Pishin belt, which are in turn bounded by the Chaman-Nushki Fault Zone (Kasi et al., 2012; UL-Hadi et al., 2013; Crupa et al., 2017). To the east, the belt is bounded by Indus Plain (Figs 1 and 2).

3. Stratigraphy

The western part of the SFTB contains over thousands of meters thick succession of sedimentary and volcanic/volcano-clastic rocks that are Triassic to Recent in age (Table 1) (Waheed and Wells, 1990; Kassi et al., 2009). Williams (1959) introduced the name Wulgai Formation for the Middle and Upper Triassic rocks, which are exposed in the SFTB. Type-locality of the Wulgai Formation is the homonimous village in Khaznozai area (Pishin District), where it is 1180 meters thick. The base of the unit is not exposed anywhere in SFTB. The formation is dominated by shale/mudstone with subordinate interbedded micritic and arenaceous limestone, and/or siltstone. The limestone is grey to dark grey, brownish grey when weathered, micritic, hard and at places recrystallised and sparitic. The limestone displays the characteristics of distal turbidites (Kassi, 1986; Kasi and Khan, 1993; Kasi and Khan, 1997) and are rhythmically interbedded with shale. The sandstones in the studied sections are light grey, thick to very thick bedded, display lenticular geometry, and have erosive bases. The sandstone is massive to trough cross-bedded and channelized. The tops of beds are mostly bioturbated. The sandstone of the Wulgai Formation occurs as thick solitary channels or as stacked channels as in Nawe Oba Section. The succession is also intruded by dolerite sills and dykes (Kerr, 2010).

The lower boundary of the formation is not exposed while the passage to the overlying Jurassic succession (i.e. Loralai Formation) is well exposed and transitional (Fatmi, 1977). The Wulgai Formation is sparsely fossiliferous. In particular, Columbites sp., has been reported in the lower part, whereas Halorites sp., Jovites sp., Pararcestes sp., Arietoceltites sp., Halobia sp. and Monotis salinaria have been reported in the upper part. On the basis of these fossils, Fatmi (1977) assigned an Early to Late Triassic age to the Wulgai Formation.

4. Material and methods

Sandstone was systematically sampled from the Wulgai Formation in various sections around the Zhob District (Figs 2 and 3). Twenty-five thin sections of fine- to medium-grained were selected for point-counting, including eight from the Zhob City Section (N 31° 20.419', E 069° 28.386') (ZCJI: Zhob City Jurassic Ismail), three from the Hassu Bandh Section (ZHJI: Zhob Hasu Band Jurassic Ismail), nine from the Nawe Oba Section (N 31° 27.036', E 069° 21.206') (ZNJI: Zhob Naweoba Jurassic Ismail) and five from the Feroz-e-Kan Section. The selected samples were point-counted using a Pelcon Automatic Point Counter, mounted on Leica DM 750 P Microscope, at the Center of Excellence in Mineralogy University of Baluchistan Quetta. One thousand points were counted in each thin section using the Gazzi-Dickinson method (Gazzi, 1966; Dickinson, 1970). The components were grouped according to the petrographic groups of Zuffa (1980). Recognition of grains was attained with the confidence of almost all grains, therefore, one thousand counts per thin section yielded statistically reliable values for all the parameters. Point-count data was recalculated to get their percentages. The components selected for point-counting include mono-crystalline quartz, poly-crystalline quartz, K-feldspar, plagioclase, micas, accessory minerals, lithic fragments (i.e. sedimentary, metamorphic, volcanic rocks) and cement, which are defined in Tables 2 and 3. In order to avoid more than one counting of larger clasts, the point counts were set at 0.4 mm and traverse at 2 mm apart.

Table 1. Stratigraphic succession of the western Sulaiman Fold-Thrust Belt.

Age	Formation	Lithology
Pleistocene	Lei Conglomerate	Conglomerate, sandstone.
Miocene-Pleistocene	Urak Group	Sandstone, claystone and conglomerate.
	Angular Unconformity	
Middle- Late Eocene	Spintangi Formation	Limestone, shale and sandstone.
Early Eocene	Ghazij Formation	Claystone, sandstone, conglomerate, limestone and coal seams.
Palaeocene	Dungan Formation	Limestone and shale.
Late Cretaceous	Pab formation / Moro Formation / Fort Munro Formation / Oxidized Transitional Succession / Hanna Lake limestone / Bibai Formation	Sandstone, siltstone, shale, limestone, *in-situ* basic volcanic rocks, volcanic conglomerate, volcanic breccia and mudstone.
Early-Middle Cretaceous	Parh Limestone / Goru Formation / Sembar Formation	Limestone (bio-micritic), marl and shale.
	Disconformity	
Jurassic	Loralai Formation	Limestone and minor shale.
Triassic	**Wulgai Formation**	**Shale, limestone and sandstone.**

5. Results

5.1 Petrology of Sandstone

The sandstone is mostly fine-grained; however, medium-grained facies occur. It is moderately to well sorted and is mostly tightly packed (Fig 4). Grains are sub-angular to well-rounded, have low sphericity (Fig. 4a), and have straight, sutured or concavo-convex contacts with each other; moreover the sandstone is mostly tightly packed (Fig 4b). The competent grains have often penetrated the incompetent grains in the tightly packed sandstone. Detrital quartz and feldspar are the most common mineral constituents. Other minerals include are muscovite, biotite, opaque minerals and heavy minerals. Various types of lithic fragment are also present. The most common cement is calcite; however, hematite and chlorite cements are also present. The main features of the mineral constituents, cements and lithic fragment are described below:

4.1.1 Quartz

Quartz is the most abundant framework grain in sandstone. It includes both mono-crystalline and poly-crystalline types but mono-crystalline quartz (Fig 4c) is very common as compared to the poly-crystalline quartz. The mono-crystalline quartz grains exhibit both undulose and non undulose extinction. Euhedral crystals of the authigenic mono-crystalline quartz have also been observed (Fig 4d). Quartz grains are commonly replaced by calcite cement, which corrodes the boundaries of the mono-crystalline quartz.

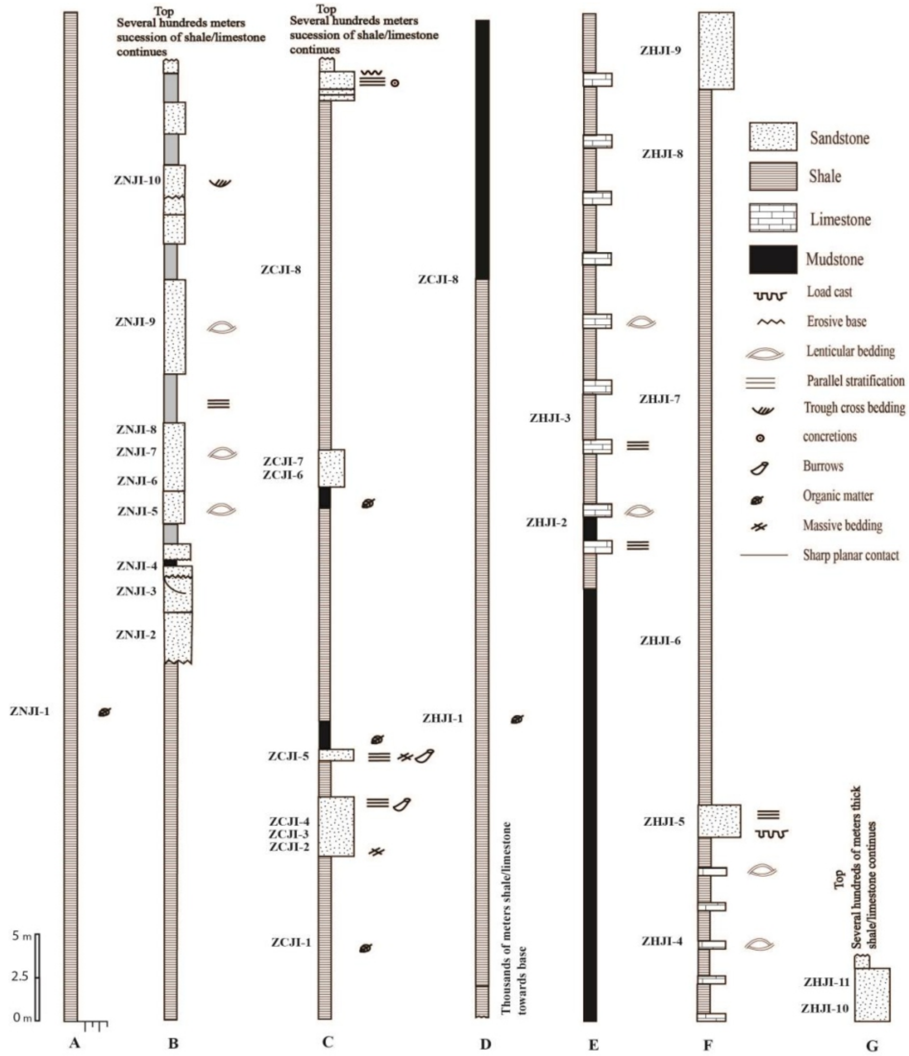

Fig. 1. Sedimentary logs showing the sandstone succession of Triassic Wulgai Formation, Zhob District. (A-B) Nawe Oba Section; (C) Zhob City Section; (D to G) Hasu Band Section.

Table 2. Detrital modes of the Triassic Wulgai Formation. Abbreviations used in the table stands for Q (Quartz), Qm (Quartz mono), Qp (Quartz poly), Qt (total quartz), F (Feldspar), P (Plagioclase), K (Potassic feldspar), L (Lithic fragments), Lt (Total lithic fragments), Lm (Meta lithics), Lv (Volcanic lithics), Ls (Sedimentary lithics), Lvm (Meta-volcanic lithics), Lsm (Meta-sedimentary lithics).

Sections and samples	Q%	F%	L%	Qm%	F%	Lt%	Qm%	P%	K%	Lm%	Lv%	Ls%	Qp%	Lvm%	Lsm%	Qt%	F%	L%
Zhob City																		
ZCJ-11	99	0.5	0.5	97.5	0.5	2.0	99	0.5	0.5	100	0	0	67	0	33	99	0.5	0.5
ZCJ-10	100	0	0.0	97	0.0	3.0	100	0	0	0	0	0	100	0	0	100	0.0	0
ZCJ-08	99.7	0	0.3	99.7	0.0	0.3	100	0	0	100	0	0	0	0	100	100	0.0	0
ZCJ-07	99.6	0	0.4	99.6	0.0	0.4	100	0	0	100	0	0	0	0	100	100	0.0	0
ZCJ-05	90	10	0	86	10	4.0	90	3	7	100	0	0	97	0	3	90	9.8	0.2
ZCJ-04	99	0.5	0.5	99	0.5	0.5	99	0.1	0.9	100	0	0	33	0	67	99	0.5	0.5
ZCJ-03	99	0.4	0.6	97	0.5	2.5	99.5	0	0.5	100	0	0	73	0	27	99	0.0	1
ZCJ-02	99.8	0	0.2	99.6	0.0	0.4	100	0	0	100	0	0	33	0	67	100	0.0	0
Zhob Newoba		-	-	-	-	-	-	-	-	-	-	-	-	-	-			
ZNJ-11	98	2	0.0	97.6	2	0.4	98	0.5	1.5	0	0	0	100	0	0	98	1.6	0.4
ZNJ-10	97	3	0.0	96	3.4	0.6	96.5	1.5	2	0	0	0	100	0	0	96.6	3.4	0.0
ZNJ-09	94	6	0.0	93	6.1	0.9	94	2.7	3.3	0	0	0	100	0	0	94	6.0	0.0
ZNJ-08	99	0.4	0.6	99	0.0	1	100	0	0	100	0	0	0	0	100	99	0.0	1
ZNJ-07	92	7.8	0.2	91	8	1	92	2	6	0	0	100	80	0	20	92	7.5	0.5
ZNJ-06	94	5.8	0.2	93	5.6	1.4	94	2.7	3.3	50	0	50	83	0	17	94	5.7	0.3
ZNJ-05	93	6.9	0.1	92	6.9	1.1	93	2	5	0	0	100	90	0	10	93	6.5	0.5
ZNJ-03	93	7	0.0	92	7.4	0.6	93	1.4	5.6	0	0	0	100	0	0	93	7.0	0.0
ZNJ-02	91	8.9	0.1	88	9	3.3	91	2.2	6.8	100	0	0	97	0	3	91	8.5	0.5
Zhob Hassu Bandh																		
ZHJ-10	99	0.9	0.1	99	0.5	0.5	99	0	0.5	0	0	100	80	0	20	99	0.5	0.5
ZHJ-09	99.8	0.2	0.0	99	0.1	0.9	100	0	0.2	0	0	0	100	0	0	99.8	0.2	0.0
ZHJ-03	93	6.9	0.1	92	6	2	93	2	5.1	100	0	0	93	0	7	93	6.5	0.5
Feroz-e-Kan																		
F-24	96	3.6	0.4	99	.5	.5	96	2	2.0	67	0	33.3	40	0	60	96	3.6	0.4
F-23	96	3.9	0.1	100	0	0	96	1	2.4	100	0	0	67	0	33	96	3.8	0.2
F-19	94	5	1	98	0	2	95	1	4	67	17	17	57	7	36	94	5	1
F-15	96	4	0.0	99	1	0	96	1	3.1	0	0	0	100	0	0	96	4	0.0
F-14	94	5.9	0.1	99	.5	.5	94	3	3.3	100	0	0	83	0	17	94	6	0
Mean	96	4	0.2	96	3	1	96	1	2	55	1	16	71	0	29	96	4	0

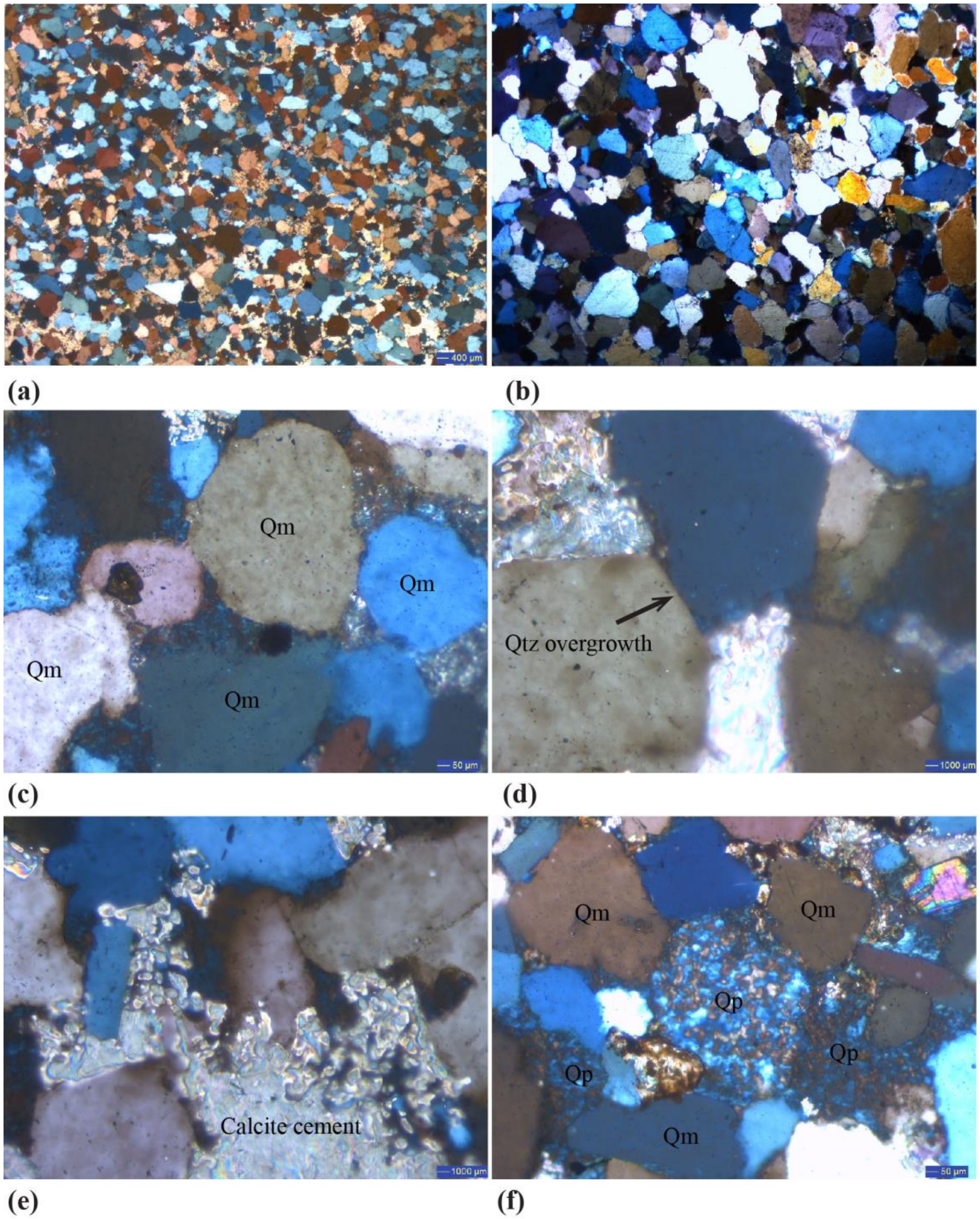

Fig. 4. Photomicrographs of sandstones of the Wulgai Formation showing a) fine-grained, subrounded and moderately sorted sandstone 10x2.5, XPL; b) tightly packed quartz grains 10x2.5 XPL; c) well rounded monocrystalline quartz grains, 10x20, XPL; d) authigenic quartz crystals, 10x40, XPL; e) replacement of quartz grains by calcite cement; f) polycrystalline quartz grains with more than three sub crystals, 10x20, XPL.

Partial to full replacement of quartz grains by calcite cement leaves behind relics of the original grains (Fig 4e). The poly-crystalline quartz is usually composed of more than three subgrains, having straight or sutured contacts (Fig 4f). Some mono-crystalline quartz grains can also show authigenic quartz overgrowth (Fig 5a). Boehm lamellae in the quartz are the sub parallel lines of very small bubbles; they are the product of intense deformation of quartz grains (Fig 5b). Some quartz grains also show strain marks. The quartz grains show mineral inclusions of rutile, tourmaline, zircon, and opaque minerals (Fig 5c and d).

4.1.2 Feldspar

The feldspar is an important mineral group in sandstone, which includes both K-feldspar and plagioclase. The feldspar was differentiated from quartz on the basis of its twining, cleavage planes and cloudy appearance, which arises from alteration. Plagioclase is more abundant than K-feldspar. K-feldspar includes perthite and orthoclase (Fig 5e), whereby the orthoclase occasionally shows Carlsbad twining while the plagioclase grains show characteristic albite-type twining (Fig 5f), low relief and oblique extinction.

4.1.3 Micas

Micas include muscovite, biotite and chlorite. The muscovite characteristically displays highly bright birefringence (Fig 6a), whereas biotite is brown to dark brown with pleochroic halos. Both have parallel extinction and moderate to variable relief. The alteration of biotite flakes to chlorite is common, in some cases they are completely chloritized. Mica flakes have regularly been squeezed, deformed and broken between competent quartz grains due to compaction (Fig 6b).

4.1.4 Accessory minerals

Heavy and opaque minerals are the main accessory minerals. The heavy minerals include rutile, tourmaline, staurolite, zircon, and hornblende. Tourmaline displays pleochroism when rotated and changes its colour from different hues of green to pink (Fig 6c). Staurolite has very high relief (Fig 6d). Hornblende is also pleochroic and varies from green to brown hues. Zircon is usually present in the form of very small crystals with high relief (Fig 6e). Tourmaline and zircon are the most common among the heavy minerals.

4.1.5 Cement

The binding material of the sandstone of the Wulgai Formation includes mainly calcite and, subordinately chlorite, hematite, clay and quartz cements. Calcite is the most common cementing material, fills the voids in the form of micrite (Fig 6f), sparite and poikilotopic calcite (Fig 7a). The calcite crystals typically exhibit rhombohedral cleavages (Fig 7a). The chlorite and clay cement usually follow the outline of quartz grain (Figs 7b and c). The quartz cement occurs in the form of authigenic overgrowth at the rim of detrital quartz (Fig 7d), and is appreciable in most of the thin sections (see Fig 7d for an example). This is particularly clear in tightly packed sandstones, where dissolution at the boundary of quartz grains resulted in overgrowth of quartz cement. Iron oxide cements coating over entire grain or along the grain margins are also frequent.

4.1.6 Lithic fragment

Rock fragments of the study sandstones, include sedimentary, igneous and metamorphic rocks. Metamorphic lithic fragments are predominant in lithic association, followed by the igneous rocks and, subordinately, by sedimentary lithics. Metamorphic lithic fragments include phyllite and schist (Fig 7e), while igneous fragments include granite and rhyolite. Chert, zebraic-chalcedony and mudstone are among the sedimentary lithics (Fig 7f).

4.2 Setrital modes3

The composition of the sandstone is primarily influenced by the composition of the source rocks, therefore, the modal analysis of the detrital framework grain is commonly used for provenance analyses (Dickinson, 1970; Dickinson and Suczek, 1979; Dickinson et al., 1983). The affiliation between the depositional basin and provenance is governed by the Plate tectonics. The compositional fields, which characterize the different provenances, are shown on the triangular diagram proposed by different authors.

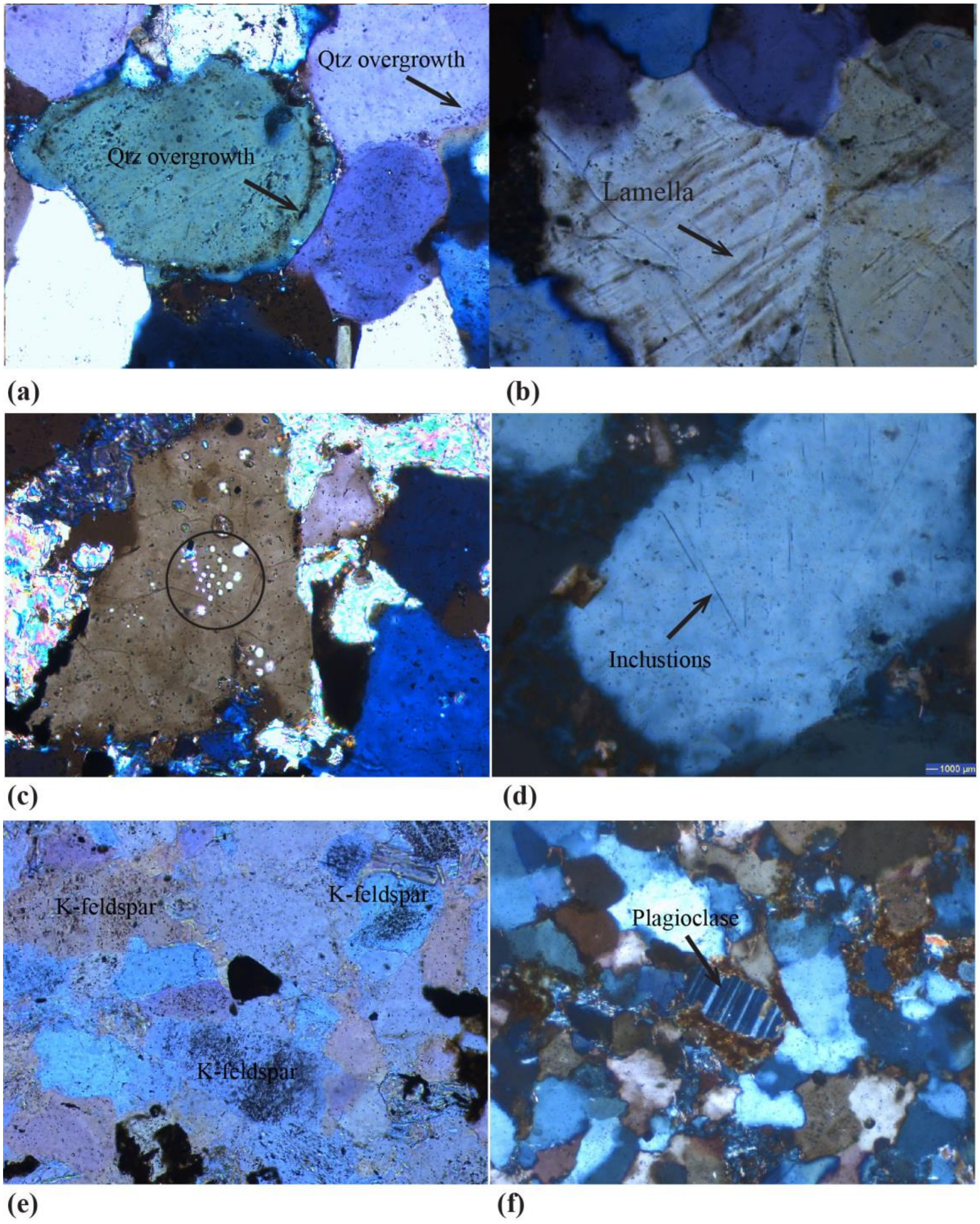

Fig. 5. Photomicrographs of sandstones of the Wulgai Formation showing; a) the authogenic overgrowth of the monocrystalline quartz, 10x20, XPL; b) boehm lamella in monocrystalline quartz, 10x20, XPL; c) mineral inclusions (encircled) in monocrystalline quartz, 10x20, XPL; d) needle-like mineral inclusion in monocrystalline quartz, 10x40, XPL; e) K-feldspar grains, 10x10, PPL; f) plagioclase feldspar showing albite-type twinning, 10x10, XPL.

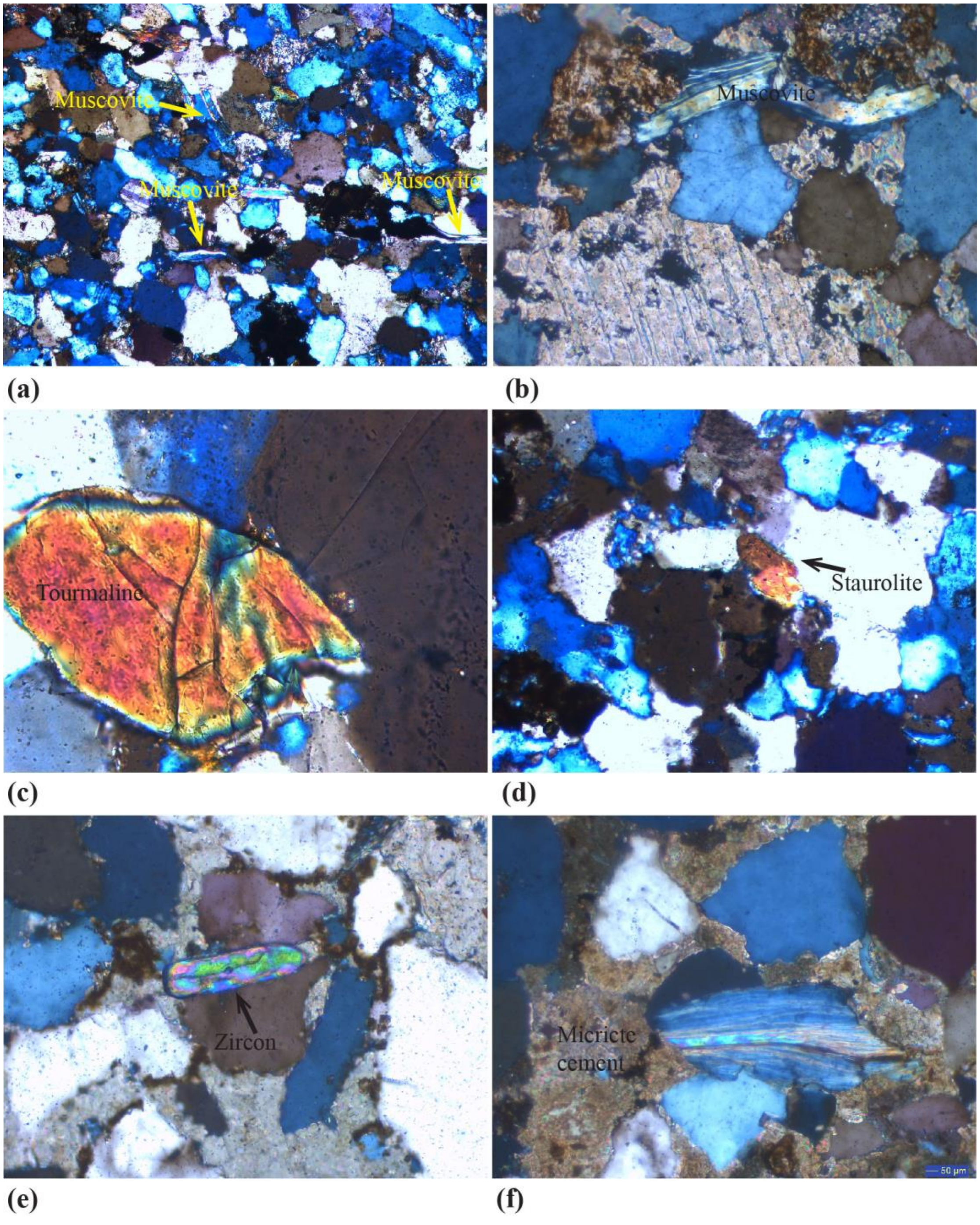

Fig. 6. Photomicrographs of sandstones of the Wulgai Formation showing; a) muscovite flakes, 10x2.5, XPL; b) a broken muscovite grain, 10x20,XPL; c) a tourmaline grain, 10x40, XPL; d) a staurolite grain 10x20, XPL; e) an elongated zircon grain, 10x20, XPL; f) microcrystalline calcite 10x20, XPL.

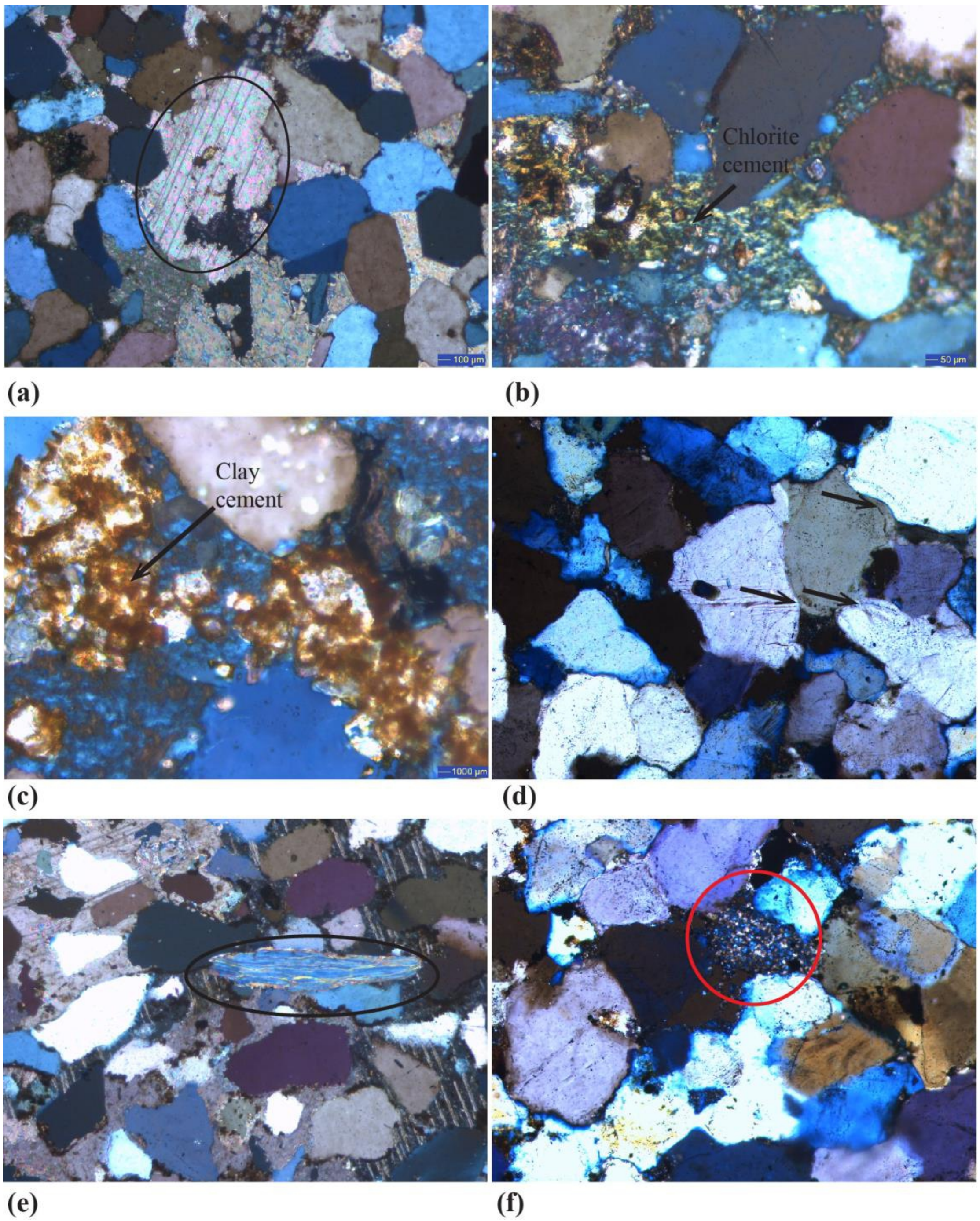

Fig. 7. Photomicrographs of sandstones of the Wulgai Formation showing; a) rhombohedral cleavages in poikilotopic calcite cement, 10x20, XPL; b) chlorite cement 10x20, XPL; c) clay cement 10x20, XPL; d) quartz cement in the form of quartz overgrowth surrounding detrital quartz (black arrows) 10x20, XPL; e) schist fragment (encircled), 10x20, XPL; f) chert fragment (encircled), 10x20, XPL.

Twenty-one recalculated parameters have been used to plot on six ternary diagrams, Q-F-L, Qt-F-L, Qm-F-Lt, Qm-P-K, Lm-Lv-Ls and Qp-Lvm-Lsm (Table 2 and 3), proposed by Dickinson and Suczek (1979), Ingersoll and Suczek (1979), Zuffa (1980), Dickinson et al. (1983), Ingersoll et al. (1984), Dickinson (1985) and Pettijohn et al. (1987). In order to classify the sandstone of the Wulgai Formation, the scheme proposed by Pettijhon et al. (1987) has been used to plot the recalculated percentages of the sample in Q-F-L ternary diagram. In this diagram the Q represents both the poly-crystalline and mono-crystalline quartz, F represents the total feldspar including K-feldspar and plagioclase feldspar, L represents the sedimentary, metamorphic and volcanic lithic fragments. The mean value is Q96F4L0.2. Most of the sandstone samples of the Wulgai Formation fall within the quartz arenite field close to the Q-F leg (Fig 8a), whereas some sample fall in the subarkose field, still close to quartz arenite field.

The Qt-F-L triangular diagram (after Dickinson and Suczek, 1979) is used for the first order classification of provenance of the sandstones. Dickinson and Suczek (1979) described three tectonic settings, continental block,

Table 3: Definitions of various grain parameters.

Q = Qm + Qp
Where Qm = monocrystalline quartz grains
Qp = polycrystalline quartz grains
Qt = Qm + Qp + C
Where Qt = total quartz grains
C = chert grains
F = P + K
Where F = total feldspar grains
P = plagioclase
K = K-feldspar grains
L = C + CF + Ls + Lm + Lv
Where L = lithic fragments
C = chert fragments
CF = carbonate fragments
Ls = sedimentary lithic fragments
Lm = metamorphic lithic fragments
Lv = volcanic lithic fragmnets
Lt = Qp + C + CF + Ls + Lm + Lv
Where Lt = total lithic fragments
Lsm = C + CF + Ls + Lm
Lvm = Lv + metavolcanic lithic fragments

Table 4: Ranges and mean values of the various minerals and rock fragments of the Triassic Wulgai Formation (western Sulaiman Fold-Thrust-Belt, Pakistan).

Components	**Triassic sandstone**	
	Range %	**Mean %**
Quartz total	45-95	76.8
Qurtz mono	44-95	76
Quartz poly	0-3.5	0.784
Feldspar total	0-9	3.104
K-feldspar	0-6.2	2.16
Plagioclase	0-0.3	0.944
Mica	0-3	0.772
Accessory Minerals	0.3-1.1	0.592
Cement	1.5-55	18.616
Rock fragments total	0-0.6	0.152
Igneous fragments	0-0.1	0.004
Sedimentary fragments	0-0.2	0.028
Metamorphic fragments	0-0.4	0.12

The continental block provenances were further subdivided by Dickinson and Suczek (1979) into three groups: craton interior, uplifted basement and transitional between craton interior and uplifted basement in Qm-F-Lt diagram. All the analyzed samples of Wulgai Formation fall into the craton interior field of the Qm-F-Lt triangle plot (Fig 9a). In particular, the mean values are Qm96F3Lt1, showing very high mono-crystalline quartz content and negligible values for lithic fragments (Lt) and feldspar (F) (see also Table 4).

The Qm-P-K triangular plot (after Dickinson, 1985) use only major mineral framework grains. The Qm-P-K plot of the sandstone show that the percentage of the monocrystalline quartz (Qm) is very high as compared to both plagioclase (P) and K-feldspar (K) and the entire samples plot near to the Qm pole, close to the Qm-K leg (Fig 9b). For the Wulgai Formation the mean values is Qm96P1K3 (Table 2).

The Lm-Lv-Ls triangular plot of Ingersoll and Suczek (1979) and Suczek and Ingersoll (1985) uses only the lithic fragments in order to classify sandstone. The Wulgai Formation is rich in metamorphic lithic fragments, and low in sedimentary and volcanic lithic fragments (mean values Lm55Lv1Ls16).

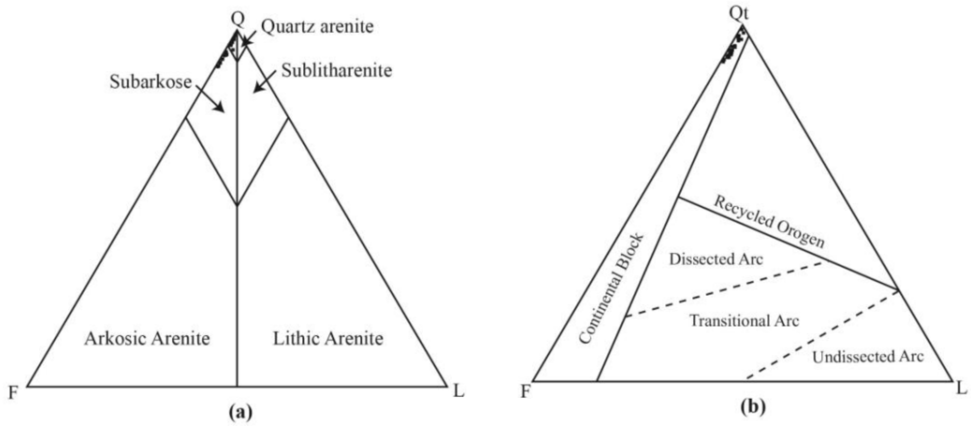

Fig 8. a) Q-F-L diagram for sandstone of the Wulgai Formation, b) tectonic provenance as shown by Qt-F-L compositional diagram for sandstone of the Wulgai Formation of the study area.

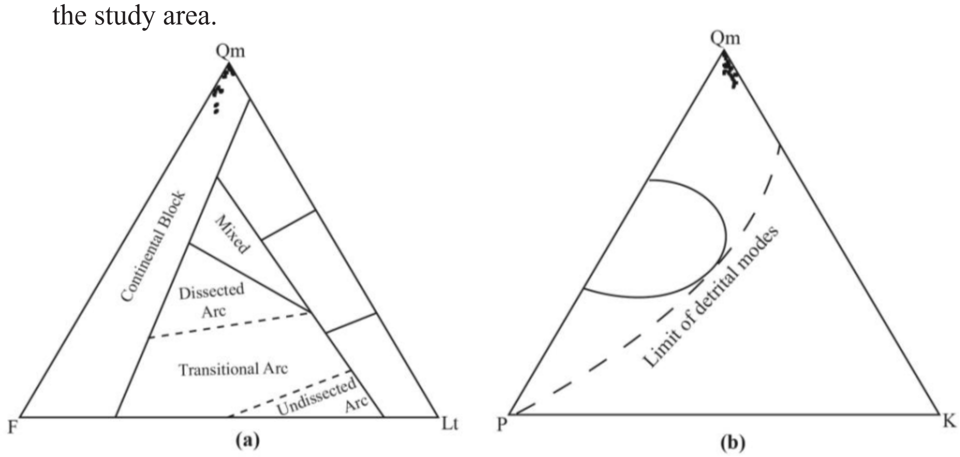

Fig 9. a) Qm-F-Lt compositional diagram of sandstone of the Wulgai Formation, b) Qm-P-K compositional diagram of sandstone of the Wulgai Formation.

The Lm-Lv-Ls triangular plot (Fig 10a) shows that most of the samples fall in the field of suture belts along the Lm-Ls leg. This plot also indicates that the lithic fragments mainly derived from metamorphic and sedimentary source rocks. The Qp-Lvm-Lsm triangular diagram (after Dickinson and Suczek, 1979; Ingersoll and Suczek, 1979; Dickinson et al. 1983) is also valuable to differentiate among the detrital modes of suture belts, magmatic arc and rifted continental margins. Qp-Lvm-Lsm triangular plot (Fig 10b) for the study sandstones shows that all the samples plot within the field of rifted continental margin. Mean values of Wulgai Formation is Qp71Lvm0Lsm29 and the samples plot along the Qp-Lsm leg (Fig 10b).

5. Provenance

The sandstone petrology of the Wulgai Formation indicates that their detritus has mainly been derived from metamorphic and igneous terrains. The high amount of monocrystalline quartz, which show non-undulose and undulose extinction, indicates that the grain derived from a plutonic igneous source (Blatt, 1967). The presence of heavy minerals such as zircon, tourmaline, staurolite and rutile also supports contribution from acidic igneous sources (Gallala et al., 2009). The Qt-F-L and Qm-F-Lt diagrams show the craton interior as source terrain for the sandstones of the Wulgai Formation. The Qm-P-K ternary diagram shows that the Wulgai Formation is rich in monocrystalline quartz and poor in feldspars, which indicate the arenite nature for the sandstone. Despite the very low content of lithic fragments in the Wulgai Formation, the latter are very essential for determining the type of source terrain for sandstones (Graham et al., 1976). For the Wulgai Formation the Lm-Lv-Ls and Qp-Lvm-Lsm plots show that the lithic detritus of the Wulgai Formation mainly derived from sedimentary and metamorphic source terrains.

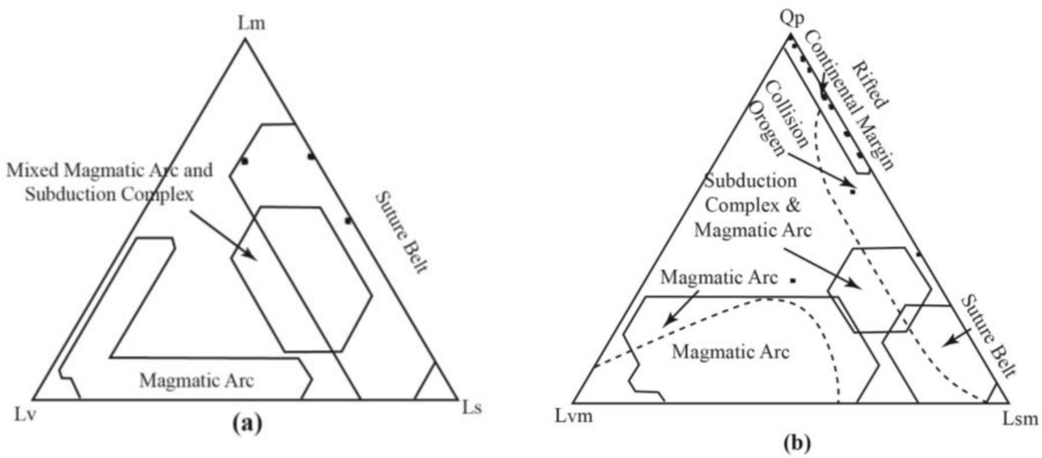

Fig 10. a) Lm-Lv-Ls diagram of the lithic component in sandstones of the Wulgai Formation; b) Qp-Lvm-Lsm compositional diagram of sandstones of the Wulgai Formation; dashed-lines indicate provenance fields of Dickinson and Suczek (1979) and solid-lines indicate provenance fields of Ingersoll and Suczek (1979).

6. Discussion

Indian Plate was part of the Gondwana super-continent during the Triassic and Jurassic periods. It started rifting from Gondwana in the Early Cretaceous (Powell et al., 1988; Norton and Sclater, 1979; Schettino and Scotese, 2005). The shield-shaped Indian Plate collided with the Eurasian Plate (Tibet) in the Eocene, after travelling northwards for 6000 km, forming the Himalayan fold and thrust belt (Lee and Lawver, 1995; Rowley, 1998; Hodges, 2000; DeCelles et al., 2002; Zhu et al., 2013; Leech et al., 2005; Szulc, A. G., 2006). The Indian Craton, which lies to the east-south east of SFTB, is believed to be the source of d`etritus for Wulgai sediments. The Indian Craton in Pakistan consists of several inliers of Precambrian basement rocks of the Kirana Group in Sargodha-Shakot area and Precambrian Nagar Parkar Igneous Complex in Nagar Parkar, Thar (Kazmi and Jan, 1997). The Kirana Group is composed of metasedimentary and metavolcanics phyllites, slates, quartzites and subordinate volcanics (Davies and Crawford, 1971). Igneous rocks of Nagar Parkar are classified into metabasites, acid dykes of rhyolite/quartz trachyte in metabasites, grey granite, pink granite and mafic dykes (Kazmi and Jan, 1997). The northwestern boundary of Indian Plate remained passive in the vast Tethys Ocean until collision (Ali and Aitchison, 2008). The Triassic Wulgai Formation and Jurassic Loralai Formation show a gradual progradational trend from deep marine to shallow marine environments and ultimately emergence, as represented by the disconformity between the Jurassic Loralai Formation and Jurassic-Lower Cretaceous Sember Formation (Kassi et al., 2009). Modal analysis of the Jurassic Loralai Formation (Manan, 2012), Late Cretaceous Pab and Mughal Kot formations in SFTB (Kassi et al., 1991; Sultan and Gipson, 1995; Sarwar, 2001) also indicates the same source for the clastic detritus of these formations. The Indian Craton remained the source terrain for the sediments of SFTB until the collision of Indian Plate with Eurasian Plate; later the emerging Himalayas became the major source of detritus to remnant parts of Neo-Tethys ocean (Qayyum et al., 2001).

7. Conclusion

Sandstone of the Wulgai Formation is fine- to medium-grained quartz arenite. Quartz and feldspars are the most common mineral constituents, monocrystalline quartz and plagioclase being abundant among them. Metamorphic lithic fragments are predominant in lithic association, followed by the igneous rocks and, subordinately, by sedimentary lithics. The Qm96F3Lt1 detrital modes indicate that sandstones of the Triassic Wulgai Formation were fed by the Craton interior. The Indian Craton, which lies to the east of Sulaiman Fold-Thrust belt, is the most likely source for the detritus of the sandstone, the sandstone was recycled enroute to reach at the destination, which was western passive margin of Indian Plate.

Acknowledgements

I would like to thanks Director Centre of Excellence in Mineralogy, University of Balochistan for providing fund and logistic for the fieldwork. I would also like to thanks Dr. Akhtar Muhammad Kassi for valuable advice during preparing this manuscript.

Authors' Contribution

Muhammad Ismail led this project in his M.Phil. and wrote the paper. Aimal Khan Kasi proposed and supervised the project in field, lab and office and undertook the responsibility of corresponding author. Razzaq Abdul Manan co-supervised the project in field and assisted in providing the thin sections of previous studies. Mohibullah Mohibullah assisted in field, write up and revision of the manuscript. Nisar Ahmed contributed by drawing high quality maps and graphics.

References

Ali, J. R., & Aitchison, J. C. 2008. Gondwana to Asia: plate tectonics, paleogeography and the biological connectivity of the Indian sub-continent from the Middle Jurassic through latest Eocene (166–35 Ma). Earth-Science Reviews, 88(3-4), 145-166.

Bannert, D., Cheema, A., Ahmed, A., Schaffer, U., 1993. The structural development of the Western Fold Belt, Pakistan. Geologisches Jahrbuch Reihe, B80, 3-60.

Barnhart, W. D., 2017. Fault creep rates of the Chaman fault (Afghanistan and Pakistan) inferred from InSAR. Journal of Geophysical Research, Solid Earth, 122, 372– 386, doi:10.1002/2016JB013656.

Beck, R. A., Burbank, D. W., Sercombe, W. J., Olson, T. L., Khan, A. M., 1995. Organic carbon exhumation and global warming during the early Himalayan collision. Geology, 23, 387-390.

Bender F, Raza H. A., 1995. Geology of Pakistan. Gebruder Borntraeger, Berlin, Germany 414.

Blatt, H., 1967. Original characteristics of clastic quartz grains. Journal of Sedimentary Research, 37, 401-424.

Brookfield, M. E., 1993. The Himalayan passive margin from Precambrian to Cretaceous times. Sedimentary Geology, 84, 1-35.

Chatterjee, S., Goswami, A., Scotese, C., 2013. The longest voyage: tectonic, magmatic, and paleoclimatic evolution of the Indian Plate during its northward flight from Gondwana to Asia. Gondwana Research 23, 238-267.

Copley, A., Avouac, J. P., Royer, J. Y., 2010. India-Asia collision and the Cenozoic slowdown of the Indian Plate: Implications for the forces driving Plate motions. Journal of Geophysical Research, 115, 1-14.

Crupa, W. E., Khan, S. D., Huang, J., Khan, A. S., Kasi, A., 2017. Active tectonic deformation of the western Indian Plate boundary: A case study from the Chaman Fault System. Journal of Asian Earth Sciences, 147, 452-468.

Davies, R. G., & Crawford, A. R., 1971. Petrography and age of the rocks of Bulland hill, Kirana hills, Sarghoda District, West Pakistan. Geological Magazine, 108(3), 235-246.

Davy, P., Cobbold, P. R., 1988. Indentation tectonics in nature and experiment. 1. Experiments scaled for gravity. Bulletin of the Geological Institute of Uppsala, 14, 129-14.

DeCelles, P. G., Robinson, D. M., Zandt, G. 2002. Implications of shortening in the Himalayan fold-thrust belt for uplift of the Tibetan Plateau. Tectonics, 21(6), 12-1.

Dickinson, W. R., 1970. Interpreting detrital modes of graywake and arkose. Journal of Sedimentary Petrology, 40, 695-707.

Dickinson, W. R., 1985. Interpreting provenance relations from detrital modes of sandstones, In: Zuffa, G. G. (Ed.) Provenance of arenites. Springer, Dordrecht, 333-361.

Dickinson, W. R., Beard, L. S., Brakenridge, G. R., Erjavec, J. L., Ferguson, R. C., Inman, K. F., Kneep, R. A., Lindberg, F. A., Ryberg, P. T., 1983. Provenance of North America Phanerozoic sandstones in relation to tectonic setting. Geological Society of America Bulletin, 94, 222-235.

Dickinson, W. R., Suczek, C. A., 1979. Plate tectonics and sSandstone composition. American Association of Petroleum Geologists Bulletin, 63, 2164-2182

Fatmi, A. N., 1977. Neocomian ammonoids from northern areas of Pakistan. Bulletin of the British Museum of Natural History, 20, 297-380.

Gallala, W., Gaied, M. E., Montacer, M., 2009. Detrital mode, mineralogy and geochemistry of the Sidi Aïch Formation (Early Cretaceous) in central and southwestern Tunisia: Implications for provenance, tectonic setting and paleoenvironment. Journal of African Earth Sciences, 53, 159-170.

Gazzi, P., 1966. Le arenarie del flysch sopra cretaceo dell'Appenninomodenese; correlazioni con il flysch di Monghidoro. Mineralogica et Petrographica Acta, 16, 69-97.

Graham, S. A., Ingersoll, R. V., Dickinson, W. R., 1976. Common provenance for lithic grains in Carboniferous sandstones from Ouachita Mountains and Black Warrior Basin. Journal of Sedimentary Research, 46, 620-632.

Haq, S. S., Davis, D. M., 1997. Oblique convergence and the lobate mountain belts of western Pakistan. Geology, 25, 23-26.

Hodges, K. V., 2000. Tectonics of the Himalaya and southern Tibet from two perspectives. Geological Society of America Bulletin, 112, 324-350.

Ingersoll, R. V., Suczek, C. A., 1979. Petrology and provenance of Neogene sand from Nicobar and Bengal Fans, DSDP sites 211 and 218. Journal of Sedimentary Petrology, 49, 1217-1228.

Ingersoll, R. V., Bullard, T. F., Ford, R. L., Grimm, J. P., Pickle, J. D., Sares, S. W., 1984. The effect of grain size on detrital modes: A test of the Gazzi-Dickinson point-counting method. Journal of Sedimentary Petrology, 54, 103-116.

Iqbal, M., Khan, M. R., 2012. Impact of Indo-Pakistan and Eurasian Plates Collision in the Sulaiman Fold Belt, Pakistan. Search and Discovery Article 50575.

Jadoon, I. A., Khurshid, A., 1996. Gravity and tectonic model across the Sulaiman fold belt and the Chaman fault zone in western Pakistan and eastern Afghanistan. Tectonophysics, 254, 89-109.

Jadoon, I. A., Lawrence, R. D., Lillie, R. J., 1994. Seismic data, geometry, evolution, and shortening in the active Sulaiman fold-and-thrust belt of Pakistan, southwest of the Himalayas. American Association of Petroleum Geologists Bulletin, 78, 758-774.

Jones, A. G., 1961. Reconnaissance geology of part of West Pakistan. A Colombo Plan Cooperative Project, Toronto, Canada: Government of Canada.

Kasi, A. K., Kassi, A. M., Umar, M., Manan, R. A., Kakar, M. I., 2012. Revised lithostratigraphy of the Pishin Belt, northwestern Pakistan. Journal of Himalayan Earth Science, 45(1).

Kassi, A.M., 1986. Sedimentology of part of the Alozai Group, Tangai area, Ziarat District, Balochistan and its implication on the 16 proposed structure of the nearby Gogai Thrust. Acta Mineralogica Pakistanica, 2, 127-133.

Kassi, A.M., Khan, A. S., 1993. The Loralai Limestone Facies around Qila Saifullah and Rud Malzai Areas, Northeast Balochistan. Geological Bulletin University of Punjab, 28, 81-91.

Kassi, A.M., Khan, A. S., 1997. Mesozoic Carbonate Turbidites of the western Sulaiman Fold-Belt Pakistan: Geology in South Asia-II, Geological Survey and Mines Bureau, Sri Lanka, Professional Paper, 161-170.

Kassi, A. M., Qureshi, A. R., Farooqui, M. A., Kakar, D. M., 1991. Petrology and the grain size characters of The Pab sandstone of parts of the Loralai and Khuzdar districts of Baluchistan. Geological Bulletin of University of Peshawar, 24, 99-108.

Kassi, A. M., Kelling, G., Kasi, A. K., Umar, M, Khan, A. S., 2009. Contrasting Late Cretaceous–Palaeocene lithostratigraphic successions across the Bibai Thrust, western Sulaiman Fold–Thrust Belt, Pakistan: Their significance in deciphering the early-collisional history of the NW Indian Plate margin. Journal of Asian Earth Sciences, 35, 435-444.

Kazmi, A. H., Jan, M. Q., 1997. Geology and tectonics of Pakistan, Graphic publishers, Pakistan 554.

Kerr, A. C., Khan, M., Mahoney, J. J., Nicholson, K. N., Hall, C. M., 2010. Late Cretaceous alkaline sills of the south Tethyan suture zone, Pakistan: initial melts of the Réunion hotspot?. Lithos, 117(1-4), 161-171.

Klootwijk, C. T., Conaghan, P. J., Nazirullah, R., de Jong, K. A., 1994. Further palaeomagnetic data from Chitral (Eastern Hindukush): evidence for an early India-Asia contact. Tectonophysics, 237, 1-25.

Lee, T. Y., Lawver, L. A. 1995. Cenozoic Plate reconstruction of Southeast Asia. Tectonophysics, 251(1-4), 85-138.

Leech, M. L., Singh, S., Jain, A. K., Klemperer, S. L., Manickavasagam, R. M., 2005. The onset of India–Asia continental collision: early, steep subduction required by the timing of UHP metamorphism in the western Himalaya. Earth and Planetary Science Letters, 234, 83-97.

Maldonado, F., Menga, J. M., Khan, S. H., Thomas, J. C., 2011. Digital geologic map and Landsat image map of parts of Loralai, Sibi, Quetta, and Khuzar Divisions, Balochistan Province, west-central Pakistan. US Geological Survey, No. 2011-1093

Manan, A. R., 2014. Sedimentology and Petrology of the Triassic-Jurassic succession, western Sulaiman Fold-Thrust belt, Pakistan, Ph.D thesis, University of Balochistan.

Manan, R. A, Kassi, A. M., Kasi, A. K., 2012. Petrology and Provenance of the sandstone channel succession within the Jurassic Loralai Formation, Sulaiman Fold-Thrust Belt, Pakistan. Journal of Himalayan Earth Sciences, 45, 1-16.

Norton, I. O, Sclater, J. G., 1979. A model for the evolution of the Indian Ocean and the breakup of Gondwanaland. Journal of Geophysical Research, 84, 6803-6830.

Pettijohn, F. J., Potter, P. E, Siever, R., 1987. Sand and Sandstone. Springer-Verlag, New York, 547.

Powell, C. M., 1979. A speculative tectonic history of Pakistan and surroundings - some constraints from the Indian Ocean, In Farah, A., DeJong, K. A. (Eds.), Geodynamics of Pakistan, Geological Survey of Pakistan, 5-24.

Powell, C. M., Roots, S. R., Veevers, J. J., 1988. Pre-breakup continental extension in East Gondwanaland and the early opening of the eastern Indian Ocean. Tectonophysics, 155, 261-283.

Qayyum M., Niem, A. R., Lawrence, R. D., 2001. Detrital modes and provenance of the Paleogene Khojak Formation in Pakistan: Implications for early Himalayan orogeny and unroofing. Geological Society of America Bulletin, 113, 320-332.

Reynolds, K., Copley, A., Hussain, E., 2015. Evolution and dynamics of a fold-thrust belt: the Sulaiman Range of Pakistan. Geophysical Journal International, 201, 683-710.

Rowley, D. B., 1998. Minimum age of initiation of collision between India and Asia north of Everest based on the subsidence history of the Zhepure Mountain section. The Journal of Geology, 106, 220-235.

Sarwar, M., 2001. Geology of the upper cretaceous succession of the area, to the west of Spera Ragha, Pishin and Ziarat Districts, Pakistan, MPhil thesis, University of Balochistan.

Schettino, A., Scotese, C. R., 2005. Apparent polar wander paths for the major continents (200 Ma to the present day): A Palaeomagnetic reference frame for global Plate tectonic reconstructions. Geophysical Journal International, 163(2), 727-759.

Searle, M. P., Parrish, R. R., Hodges, K. V., Hurford, A., Ayres, M. W., Whitehouse, M. J. 1997. Shisha Pangma leucogranite, south Tibetan Himalaya: field relations, geochemistry, age, origin, and emplacement. The Journal of Geology, 105(3), 295-318.

Suczek, C. A., Ingersoll, R. V., 1985. Petrology and provenance of Cenozoic sand from the Indus Cone and the Arabian Basin, DSDP Sites 221, 222, and 224, Journal of Sedimentary Petrology, 55, 340-346.

Sultan, M., Gipson, Jr. M., 1995. Reservoir potential of the Maastrichtian Pab Sandstone in the Eastern Sulaiman Fold-Belt, Pakistan. Journal of Petroleum Geology, 18, 309-328.

Szulc, A. G., Najman, Y., Sinclair, H. D., Pringle, M., Bickle, M., Chapman, H., ... & Ojha, T. 2006. Tectonic evolution of the Himalaya constrained by detrital 40Ar–39Ar, Sm–Nd and petrographic data from the Siwalik foreland basin succession, SW Nepal. Basin Research, 18(4), 375-391.

Ul-Hadi, S, Khan, S. D., Owen, L. A., Khan, A. S., Hedrick, K. A., Caffee, M. W., 2013.

Slip-rates along the Chaman fault: Implication for transient strain accumulation and strain partitioning along the western Indian Plate margin. Tectonophysics, 608, 389-400.

Umar, M., Khan, A. S., Kelling G., Kassi, A. M., 2011. Depositional environments of Campanian–Maastrichtian successions in the Kirthar Fold Belt, southwest Pakistan: Tectonic influences on Late Cretaceous sedimentation across the Indian passive margin. Sedimentary Geology, 237, 30-45.

Waheed, A., Wells, N. A., 1990. Changes in paleocurrents during the development of an obliquely convergent Plate boundary (Sulaiman fold-belt, southwestern Himalayas, west-central Pakistan). Sedimentary Geology, 67, 237-261.

Williams, M. D., 1959. Stratigraphy of the lower Indus Basin, West Pakistan, Proceeding of the 5th World Petroleum Congress, New York 19: 377-390.

Zhu, D. C., Zhao, Z. D., Niu, Y., Dilek, Y., Hou, Z. Q., Mo, X. X. 2013. The origin and pre-Cenozoic evolution of the Tibetan Plateau. Gondwana Research, 23(4), 1429-1454.

Zuffa, G. G., 1980. Hybrid arenites: their composition and classification. Journal of Sedimentary Petrology, 50, 21-29.